

# Synthetic and Spectroscopic Investigations Enabled by Modular Synthesis of Molecular Phosphaalkyne Precursors

Wesley J. Transue,<sup>†</sup> Junyu Yang,<sup>†</sup> Matthew Nava,<sup>†</sup> Ivan V. Sergeyev,<sup>‡</sup> Timothy J. Barnum,<sup>†</sup> Michael C. McCarthy,<sup>¶</sup> and Christopher C. Cummins\*,<sup>†</sup>

<sup>†</sup>Department of Chemistry, Massachusetts Institute of Technology, Cambridge, MA 02139, USA

<sup>‡</sup>Bruker BioSpin Corporation, Billerica, MA 01821, USA

<sup>¶</sup>Harvard-Smithsonian Center for Astrophysics, Cambridge, MA 02138, USA

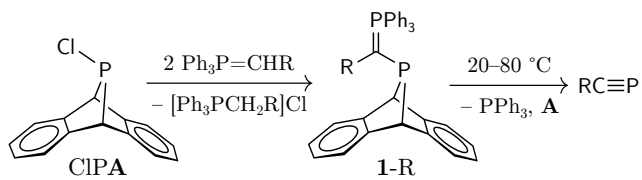
Received October 27, 2018; E-mail: ccummins@mit.edu

**Abstract:** A series of dibenzo-7-phosphanorbornadiene compounds,  $\text{Ph}_3\text{PC}(\text{R})\text{PA}$  (**1-R**;  $\text{A} = \text{C}_{14}\text{H}_{10}$ , anthracene;  $\text{R} = \text{Me}$ ,  $\text{Et}$ ,  $^i\text{Pr}$ ,  $^s\text{Bu}$ ), are reported to be capable of thermal fragmentation to generate alkyl-substituted phosphaalkynes ( $\text{RC}\equiv\text{P}$ ) concomitant with triphenylphosphine and anthracene. Facile preparation of these molecular precursors proceeds by treatment of **CIPPA** with the appropriate ylide  $\text{Ph}_3\text{P}=\text{CHR}$  (2 equiv). For methyl, ethyl, and isopropyl substituents, the phosphaalkyne conversions are measured to be 56–73% in solution by quantitative  $^{31}\text{P}$  NMR spectroscopy. In the case of compound **1-Me**, the kinetic profile of its spontaneous unimolecular fragmentation is investigated by an Eyring analysis. The resulting 1-phosphapropyne is directly detected by solution NMR spectroscopy and gas phase rotational microwave spectroscopy. The latter technique allows for the first time measurement of the phosphorus-31 nuclear spin-rotation coupling tensor. The nuclear spin-rotation coupling provides a link between rotational and NMR spectroscopies, and is contextualized in relation to the chemical shift anisotropy.

## Introduction

Phosphaalkynes are a well known class of low-coordinate  $\lambda^3$ -phosphines, especially as building blocks in organophosphorus chemistry.<sup>1</sup> They have been extensively used in the synthesis of both coordination complexes and phosphines, and have a rich and useful cycloaddition chemistry.<sup>2–4</sup> The earliest reports of their synthesis relied on aggressive experimental conditions involving electric discharge<sup>5</sup> or high (900 °C) temperatures,<sup>6</sup> but milder preparations have since been developed<sup>7–13</sup> and have spurred numerous synthetic<sup>14–17</sup> and spectroscopic studies.<sup>6,18–24</sup> In pursuit of new and mild methods for generation of low-coordinate phosphorus species, we have recently reported the synthesis and thermal behavior of  $\text{Ph}_3\text{PC}(\text{H})\text{PA}$  (**1-H**;  $\text{A} = \text{C}_{14}\text{H}_{10}$  or anthracene), a compound demonstrated to fragment into phosphaethyne ( $\text{HC}\equiv\text{P}$ ), triphenylphosphine, and anthracene upon mild heating (80 °C).<sup>25</sup> The gradual release of HCP at elevated temperature from this precursor enabled its 1,3-dipolar cycloaddition with azide, unavailable through more traditional low-temperature manipulation techniques due to competitive polymerization.

From our further studies on phosphaalkyne generation with this platform, we now report the synthesis and thermal behavior of a series of alkyl-substituted  $\text{Ph}_3\text{PC}(\text{R})\text{PA}$  (**1-R**;  $\text{R} = \text{Me}$ ,  $\text{Et}$ ,  $^i\text{Pr}$ ,  $^s\text{Bu}$ ) compounds. In contrast to **1-H**,



**Scheme 1.** Synthesis and fragmentation of alkyl-substituted phosphaalkyne molecular precursors,  $\text{Ph}_3\text{P}=\text{C}(\text{R})\text{PA}$  (**1-R**;  $\text{R} = \text{H}$ ,  $\text{Me}$ ,  $\text{Et}$ ,  $^i\text{Pr}$ ,  $^s\text{Bu}$ ;  $\text{A} = \text{C}_{14}\text{H}_{10}$ ).

**H**, **1-R** compounds have been found to spontaneously release the  $\text{RC}\equiv\text{P}$  payload into solution at or below room temperature. This series of phosphaalkyne precursors has allowed us to pursue further exploratory reactivity and spectroscopic studies of  $\text{RC}\equiv\text{P}$  compounds, underscoring the value of the molecular precursor approach to accessing the chemistry of reactive intermediates.

## Results and Discussion

### Substituent Investigations

Interested in expanding the scope of **1-R** compounds beyond the phosphaethyne precursor, we set out to synthesize analogs with alkyl substituents. We envisioned access to these  $\text{RC}\equiv\text{P}$  precursors through treatment of **CIPPA** with an appropriate Wittig reagent (Scheme 1), the same synthetic route as devised for **1-H**.<sup>25</sup> Accordingly, treatment of a thawing THF solution of **CIPPA** with a thawing, orange THF solution of  $\text{Ph}_3\text{P}=\text{CHMe}$ <sup>26</sup> (2 equiv) gave rapid bleaching and formation of ethyltriphenylphosphonium chloride as a colorless precipitate. Analysis of the supernatant by  $^{31}\text{P}\{^1\text{H}\}$  NMR spectroscopy revealed a pair of doublet resonances with chemical shifts of  $\delta$  197 ( $\text{P}_{\text{bridge}}$ ) and 28 ppm ( $\text{P}_{\text{ylide}}$ ) with a scalar coupling of  $^2J_{\text{PP}} = 173.0$  Hz, consistent with successful formation of **1-Me**. Repetition in  $\text{THF}-d_8$  and rapid acquisition of a series of one- and two-dimensional NMR spectra at 0 °C allowed this new species to be confidently assigned as **1-Me**.

The low temperature used in these NMR studies was necessary due to the instability of the precursor at ambient temperatures, spontaneously fragmenting to form 1-phosphapropyne. The dramatic decrease of precursor stability upon alkyl substitution had not been anticipated, but it paralleled the behavior of  $\text{R}_2\text{NPA}$  compounds, which fragment more easily with increasingly large alkyl groups.<sup>30</sup> The fragmentation of **1-R** at 25 °C was also remarkable as it allowed direct observation of the resultant  $\text{MeC}\equiv\text{P}$  by NMR spectroscopy ( $^{31}\text{P}\{^1\text{H}\}$   $\delta$   $-64$  ppm),<sup>12,28</sup> a consequence of the

**Table 1.** Phosphaalkyne  $^{31}\text{P}$  NMR chemical shifts and percent conversion from **1-R** precursors in THF solution after 2 h at 22 °C.<sup>a</sup>

R	$\delta$ / ppm	Conversion <sup>b</sup>
H <sup>12,25</sup>	-32.0 <sup>27</sup>	— <sup>c</sup>
Me	-63.5 <sup>12</sup>	56%
Et	-64.5 <sup>12</sup>	73%
<i>i</i> Pr	-65.7 <sup>28</sup>	58%
<sup>s</sup> Bu	-61.2	13%
<sup>t</sup> Bu	— <sup>d</sup>	— <sup>d</sup>

<sup>a</sup> After 2 h at 22 °C, complete consumption of all **1-R** compounds was observed by NMR spectroscopy. <sup>b</sup> Quantified by inverse-gated decoupled  $^{31}\text{P}\{^1\text{H}\}$  NMR spectroscopy after 2 h at 22 °C by integration against  $\text{PPh}_3$  with a recycle delay of at least 8T<sub>1</sub> using  $\text{Cr}(\text{acac})_3$  as a relaxation reagent.<sup>29</sup> <sup>c</sup> No appreciable fragmentation at 22 °C over 2 h. <sup>d</sup> Not observed.

increased solution stability of this phosphaalkyne in relation to  $\text{HC}\equiv\text{P}$ . Although anthracene and triphenylphosphine were released quantitatively, the conversion to 1-phosphapropyne was found to be 56% after allowing development of the solution for 2 h at 25 °C by quantitative integration against  $\text{PPh}_3$  using  $\text{Cr}(\text{acac})_3$  as a paramagnetic relaxation reagent.<sup>29</sup> The fate of the rest of the phosphorus was not obvious, and has not been tracked down.

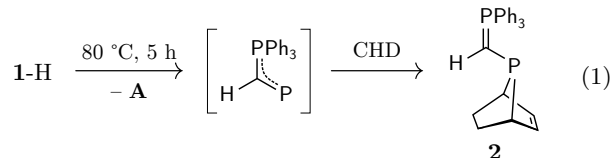
Successful phosphaalkyne generation was not limited to  $\text{MeC}\equiv\text{P}$  from **1-Me**. Further investigations into alkyl substituents have also revealed **1-Et** and **1-*i*Pr** and **1-<sup>s</sup>Bu** to fragment over 2 h at 22 °C to provide solutions of 1-phospha-1-butyne ( $\text{EtC}\equiv\text{P}$ ) and 3-methyl-1-phospha-1-butyne ( $\text{iPrC}\equiv\text{P}$ ) and 3-methyl-1-phospha-1-pentyne ( $\text{BuC}\equiv\text{P}$ ), respectively (Table 1). The percent conversion rose upon switching from a methyl to an ethyl substituent; however, further increases in steric bulk were deleterious to phosphaalkyne production. Attempts to form  $\text{tBuC}\equiv\text{P}$  through **1-<sup>t</sup>Bu** failed as  $\text{ClPA}$  was not found to react with  $\text{Ph}_3\text{P}=\text{C}(\text{H})\text{tBu}$  under our conditions, likely a consequence of the steric demands of a *tert*-butyl substituent.

### Mechanistic Insight

Density functional theory (DFT) calculations using ORCA 4.0<sup>31,32</sup> with the M06-2X functional,<sup>33</sup> Def2-TZVP basis set,<sup>34,35</sup> and RIJCOSX appromation<sup>36,37</sup> uncovered an identical mechanism for phosphaalkyne release along the closed-shell singlet potential energy surface (PES) to that reported for **1-H** (Figure 1).<sup>25</sup> This mechanism involves an initial [1,3]-sigmatropic shift of the phosphorus bridge from a norbornadiene to an intermediate norcaradiene ge-

ometry.<sup>38</sup> Such a shift could occur through a closed-shell intermediate or though an open-shell intermediate akin to [1,3]-sigmatropic alkyl shifts.<sup>39</sup> Subsequent rate-limiting [2+1]-cheletropic cycloelimination releases an unusual ylide-substituted phosphinidene intermediate from the anthracene platform. Rapid fragmentation of this ylide provides triphenylphosphine and 1-phosphapropyne.

Alternative fragmentation sequences include initial triphenylphosphine release or a single-step coarctate<sup>40</sup> mechanism. We are now in a position to provide experimental support for initial anthracene release to generate a phosphinidene. Heating **1-H** in the presence of excess 1,3-cyclohexadiene (CHD) to 80 °C for 3 h resulted in the detection of a new species identified as **2** by a series of NMR experiments (eq 1, SI §S.1.5).



Product **2** suggested direct capture of the intermediate phosphinidene to produce a new 7-phosphanorbornene framework. Initial  $\text{PPh}_3$  release would be expected to retain the dibenz-7-phosphanorbornadiene unit to produce a norbornen-7-yl substituted **RPA** compound. Single-step coarctate fragmentation would similarly not produce **2**, instead proceeding directly to  $\text{HC}\equiv\text{P}$  from **1-H** without an intermediate for interception by 1,3-cyclohexadiene.

Experimental investigations of the kinetic profile of **1-Me** decay were consistent with the mechanism proposed in Figure 1. Unimolecular decomposition of **1-Me** was observed in THF solution, and proceeded with a half life of 12.5(6) min at 25 °C. An Eyring analysis (Figure S.21) revealed kinetic parameters for this fragmentation of  $\Delta H^\ddagger = 23.0(9)$  kcal/mol and  $\Delta S^\ddagger = 4.6(3.1)$  cal/mol·K. This barrier to fragmentation was nicely in agreement with the DFT predictions, and smaller than that previously determined for **1-H** ( $\Delta H^\ddagger = 25.1(8)$  kcal/mol and  $\Delta S^\ddagger = -3.6(2.2)$  cal/mol·K),<sup>25,41</sup> as expected from the observed decrease in stability of **1-Me**.

### Bonding Analysis

The diminished barrier to fragmentation observed for **1-Me** in comparison to **1-H** likely results from an increased  $\pi$ -donicity of the ylide carbon lone pair due to the  $\alpha$ -alkyl group, mirroring the behavior of dialkylamide-substituted  $\text{R}_2\text{NPA}$  compounds.<sup>30</sup> This electronic effect can be under-

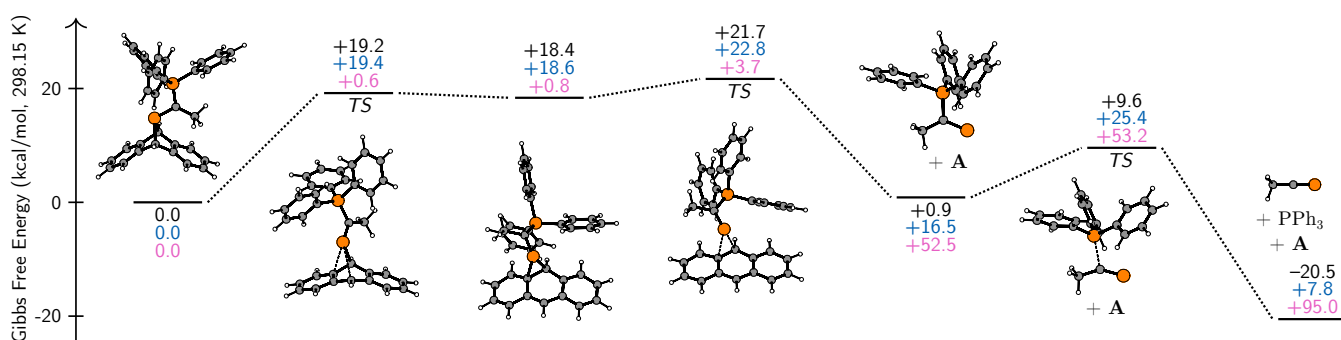


**Figure 1.** Computed mechanism of  $\text{MeC}\equiv\text{P}$  release from **1-Me** plotted as a function of the Gibbs free energy (kcal/mol, 298.15 K, black) of each intermediate and transition state (TS) along with the relative enthalpy (kcal/mol, blue) and entropy (cal/mol·K, pink).

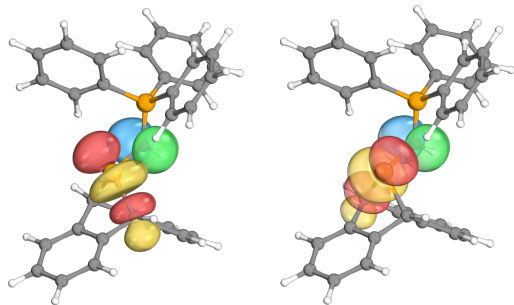


**Figure 2.** Donor-acceptor interactions between the ylidic carbon lone pair and the  $\sigma_{PC}^*$  antibonds destabilize the molecular precursors as depicted by the overlaps between these NBOs.

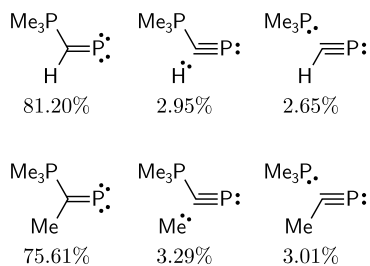


**Chart 1.** Natural resonance theory (NRT) analysis of model phosphinidenes  $[\text{Me}_3\text{P}=\text{C}(\text{R})\text{P}]$  ( $\text{R} = \text{H}, \text{Me}$ ) shows increased hyperconjugation in the methyl derivative. The phosphinidene PC natural bond orders were nearly identical: 2.02 ( $\text{R}=\text{H}$ ) and 1.99 ( $\text{R}=\text{Me}$ ).

stood in terms of a donor-acceptor interaction between the ylide lone pair and the  $\sigma_{PC}^*$  antibonds of the phosphorus and the anthracene bridgehead carbon centers. Natural bond orbital (NBO)<sup>42</sup> analysis substantiates this by quantifying the net strength of the donor-acceptor interactions to be 29.1 kcal/mol in **1-H** and 32.0 kcal/mol in **1-Me** (Figure 2). This difference of 2.9 kcal/mol matches well with the decrease in experimental enthalpic barriers:  $\Delta\Delta H^\ddagger = 2.1$  kcal/mol. The larger size of the alkyl groups of **1-R** compounds also presumably increases the steric pressure of the substituent against the anthracene scaffold, destabilizing the molecular precursor.

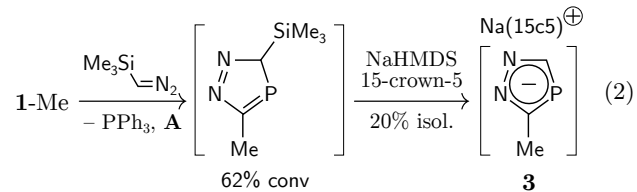
The alkyl group was also found to have an impact on the stability of the intermediate phosphinidene. In the same way that strongly donating amino and phosphino substituents play a large role in stabilization of phosphinidenes, the ylidic carbon-centered lone pair stabilizes the phosphinidene by  $\pi$ -donation into the formally empty phosphorus *p*-orbital, allowing the subvalent center to achieve an octet of electrons. The natural resonance theory (NRT) subroutine of NBO reveals this interaction to be strong enough in model species  $[\text{Me}_3\text{P}=\text{C}(\text{R})\text{P}]$  that a  $\text{P}=\text{C}$  double bond is involved in an accurate Lewis representation of the phosphinidene (Chart 1), reminiscent of *N*-heterocyclic carbenes (NHCs), aminophosphinidenes,<sup>30</sup> and phosphinophosphinidenes.<sup>43</sup> This Lewis structure is also appealing, as it emphasizes the growth of one PC bond order at the expense of the other *en route* to the final phosphaalkyne.

### Reactivity Studies

Having established the ability of these compounds to deliver simple phosphaalkynes into solution, we sought to demonstrate their utility in synthesis. Our initial report demonstrated successful 1,3-dipolar cycloaddition of  $\text{HC}\equiv\text{P}$  directly with azide to yield the previously unknown par-

ent 1,2,3,4-phosphatriazolate anion, mimicking formation of  $\text{P}_2\text{N}_3^{-44}$  and triazolate<sup>45</sup> heterocycles with  $\text{P}_2$  and acetylene, respectively. The success of this reaction was found to rely on gradual delivery of  $\text{HC}\equiv\text{P}$  to azide from **1-H** at elevated temperature, as vacuum transfer of HCP onto a frozen slurry of  $[\text{TBA}][\text{N}_3]$  (TBA = tetra-*n*-butylammonium) gave polymerization.<sup>5,46,47</sup>

Solutions of  $\text{MeC}\equiv\text{P}$  produced from **1-Me** also allowed for reactivity studies. Addition of (trimethylsilyl)diazomethane (1 equiv) to a thawing THF solution of  $\text{MeC}\equiv\text{P}$  gave 62% conversion to a [3+2] cycloadduct, isolated in 20% yield as a sodium 15-crown-5 salt **3** (eq 2) after addition of NaHMDS (0.5 equiv) and 15-crown-5 (0.6 equiv).



### Rotational Spectroscopy

As **1-H** was found to be a useful source of  $\text{HC}\equiv\text{P}$  for microwave rotational spectroscopy, we anticipated utility of **1-R** compounds for spectroscopic investigations. We selected **1-Me** as a good precursor for use in microwave spectroscopy studies because the resulting MeCP is a prolate symmetric rotor of modest size. Additionally, 1-phosphapropyne has been previously characterized by rotational and vibrational spectroscopy,<sup>48–50</sup> and its reported rotational constants<sup>6,21,51</sup> allowed prediction of the transition frequencies within the range of our microwave spectrometer (5–40 GHz). A stream of neon bubbled through a THF solution of 1-phosphapropyne from **1-Me** carried volatile 1-phosphapropyne into the instrument cavity, at which point gas expansion provided rapid cooling to *ca.* 10 K. Several rotational transitions were observed, including the  $J = 2 \leftarrow 1$  and  $J = 1 \leftarrow 0$  transitions, which were measured for the first time in this study and complement Kroto's early investigations.<sup>21</sup>

The resolution of these spectra has also allowed measure-

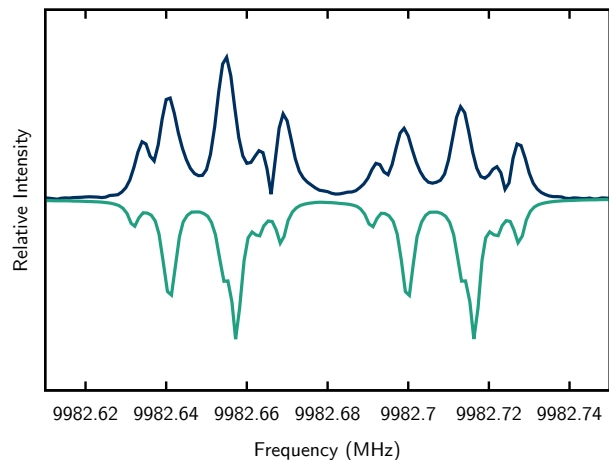


**Figure 3.** The observed  $J = 1 \leftarrow 0$  transition for 1-phosphapropyne showing hyperfine structure from nuclear spin-rotation coupling, dipolar spin-spin coupling, and Doppler doubling due to expansion of the molecular beam along the microwave excitation axis. A simulated spectrum using fitted coupling constants is shown inverted.

ment of the hydrogen-hydrogen dipolar spin-spin coupling constant and the phosphorus-31 nuclear spin-rotation coupling tensor (Figure 3). The dipolar coupling was fitted to be  $D_{HH} = 21.2(1.0)$  kHz, matching the expected value of 20.6(3) kHz based on the known microwave structure of  $\text{MeC}\equiv\text{P}$ .<sup>21</sup> The hydrogen–phosphorus dipolar coupling was not resolved, not unexpected as a magnitude of only  $D_{HP} = 1.112(8)$  kHz is expected from the microwave structure.<sup>21</sup> As a prolate symmetric rotor,  $\text{MeC}\equiv\text{P}$  has two independent components of the phosphorus-31 spin-rotation coupling tensor. The perpendicular component was fitted to be  $C_{\perp}(^{31}\text{P}) = -10.76(48)$  kHz, while the lower resolution of the observed  $K > 0$  transitions only allowed the order of magnitude of  $C_{\parallel}(^{31}\text{P})$  to be established confidently, giving  $-20(15)$  kHz. These values showed close agreement with the predicted values of  $C_{\perp} = -9.86$  kHz and  $C_{\parallel} = -20.59$  kHz at the CCSD(T)/cc-pwCVTZ<sup>52,53</sup> level of theory as calculated with CFOUR.<sup>54</sup>

The  $^{31}\text{P}$  nuclear spin-rotation coupling provides a unique link between rotational and NMR spectroscopies.<sup>55</sup> This link arises from the induced magnetic field from electronic motion in the rotationally excited molecule that interacts with the spin-1/2  $^{31}\text{P}$  nucleus similarly to an applied external field in NMR spectroscopy.<sup>56</sup> In Ramsey's formalism of nuclear magnetic shielding,<sup>57</sup> the magnetic shielding tensor comprises a diamagnetic and a paramagnetic component,  $\sigma = \sigma^{\text{dia}} + \sigma^{\text{para}}$ .<sup>58,59</sup> Nuclear spin-rotation coupling constants relate to this latter component, which results from mixing of ground and excited electronic states.

Using Flygare's approximation for diamagnetic nuclear shielding, the nuclear spin-rotation coupling tensor  $C$  can be simply related to the total nuclear magnetic shielding tensor  $\sigma$  for the phosphorus-31 center by

$$\sigma_{xx}(\text{P}) = \sigma_{\text{atom}}(\text{P}) + \frac{m_p}{2m_e g_P} \frac{C_{xx}}{B_{xx}},$$

where  $\sigma_{\text{atom}}(\text{P})$  is the diamagnetic nuclear shielding of a free phosphorus-31 atom,<sup>63</sup>  $m_p$  is the proton mass,  $m_e$  is the electron mass,  $g_P$  is the phosphorus-31 nuclear  $g$  factor,  $C_{xx}$  is the spin-rotation coupling constant along axis  $x$ , and  $B_{xx}$  is the rotational constant along axis  $x$ .<sup>55,64–66</sup> For elements other than hydrogen, the accuracy of this approximation stems from the fact that the diamagnetic component is dominated by core electrons; thus, it changes little between molecules and is approximately isotropic.<sup>67</sup> The nuclear magnetic shielding is linearly related to the more familiar NMR chemical shift scale when reported relative to a reference compound,  $\delta = (\sigma_{\text{ref}} - \sigma)/(1 - \sigma_{\text{ref}})$ .

The phosphorus-31 nuclear shielding tensor obtained from the experimentally determined spin-rotation coupling tensor was  $\sigma_{\perp} = 86(39)$  ppm,  $\sigma_{\parallel} = 909(38)$  ppm,  $\sigma_{\text{iso}} = 360(22)$  ppm. These matched well those predicted by CCSD(T)/cc-pwCVTZ calculations:  $\sigma_{\perp} = 158$  ppm,  $\sigma_{\parallel} = 916$  ppm,  $\sigma_{\text{iso}} = 410$  ppm. The absolute  $^{31}\text{P}$  nuclear shielding of 85%  $\text{H}_3\text{PO}_4$  (328.35 ppm) can be used as a reference to convert these numbers into more familiar chemical shift terms.<sup>68</sup> Thus, the chemical shift tensor was found to be  $\delta_{\perp} = 243(39)$  ppm,  $\delta_{\parallel} = -581(38)$  ppm,  $\delta_{\text{iso}} = -32(22)$  ppm. These values indicate a span of the chemical shift tensor of  $\Omega = \delta_{\perp} - \delta_{\parallel} = 824(54)$  ppm for gaseous 1-phosphapropyne in its ground state.

The large span of the tensor comports with those measured for other phosphaalkynes and related species,<sup>69,70</sup> and it is of the same order of magnitude as the spans calculated

from the nuclear spin-rotation tensors of  $\text{MeC}\equiv\text{P}$ ,  $\text{HC}\equiv\text{P}$ , and  $\text{N}\equiv\text{P}$  (Table 2). It arises from the small energy gap between the P–C  $\sigma$ -bond and the CP  $\pi^*$ -antibonds.<sup>70</sup>

### Solid-State NMR Studies

To make this link between the nuclear spin-rotation coupling tensor and the chemical shift tensor more explicit, we sought to corroborate the span by solid-state NMR spectroscopy. This was complicated by the simple fact that  $\text{MeCP}$  is not a stable solid under ambient conditions. 1-Adamantyl phosphaacetylene was selected as a  $C_{3v}$ , alkyl-substituted, and solid model phosphaalkyne. The  $^{31}\text{P}$  magic angle spinning (MAS) SSNMR spectrum at 106 K showed a series of resonances that allowed the CSA to be modeled to be  $\delta_{11} = \delta_{22} = 87.09(21)$  ppm,  $\delta_{33} = -370.24(21)$  ppm, indicating an isotropic shift of  $\delta_{\text{iso}} = -65.35(21)$  ppm and a span of  $\Omega = 457.33(30)$  ppm (Figure 4a). At 294 K, the spectrum displayed significant broadening for each spikelet, likely an effect of crystalline plasticity permitting molecular motion. The related compound  $^1\text{AdC}\equiv\text{N}$  is known to exist as a plastic crystal at room temperature<sup>71</sup> that cools into a glassy solid below 178 K.<sup>72</sup> At ambient temperatures,  $^1\text{AdC}\equiv\text{N}$  undergoes rapid rotation around its  $C_3$  axis and rapid reorientation of the molecular  $C_3$  axis among the six directions of its cubic lattice.<sup>73</sup> Similar behavior undoubtedly affects  $^1\text{AdC}\equiv\text{P}$ . Indeed, significant narrowing of each spikelet is observed upon cooling from 294 to 103 K, indicating that some but not all dynamical modes have been “frozen out.”

Such a tensor showed a marked decrease in span in comparison both with the experimental values from rotational spectroscopy and with the predicted  $^1\text{AdCP}$  tensor at the

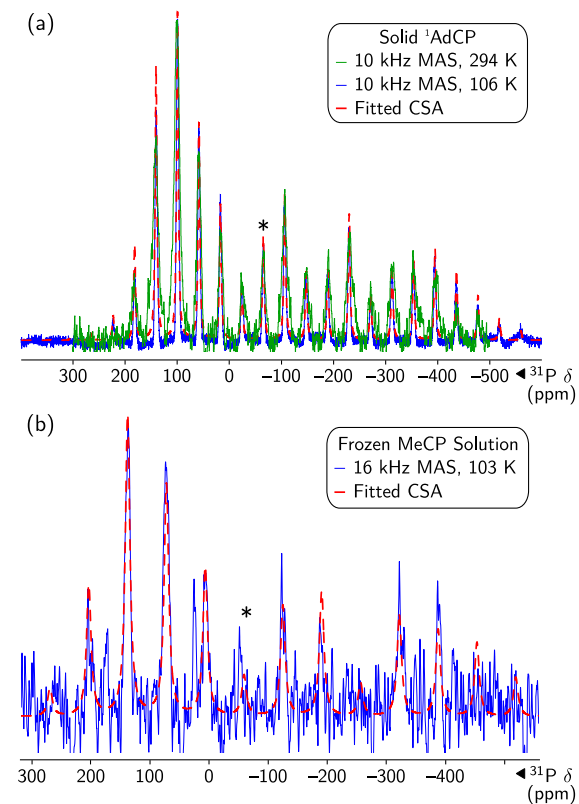


**Figure 4.** Observed and simulated  $^{31}\text{P}$  MAS SSNMR spectra of (a) solid  $^1\text{AdCP}$  and (b) a frozen toluene solution of MeCP at 242 MHz. The isotropic bands are marked with an asterisk (\*).

**Table 2.** Rotational constants, nuclear spin-rotation coupling constants, absolute nuclear shieldings, and chemical shifts for  $^{31}\text{P}$  nuclei in a series of related compounds with uncertainties listed at the  $1\sigma$  value.

Compound	Spin-Rotation Coupling		Nuclear Shielding <sup>a</sup>		Chemical Shift <sup>a</sup>			
	$C_{\parallel}^b$	$C_{\perp}^b$	$\sigma_{\parallel}^c$	$\sigma_{\perp}^c$	$\delta_{\parallel} = \delta_{33}^c$	$\delta_{\perp} = \delta_{11,22}^c$	$\delta_{\text{iso}}^c$	$\Omega^{c,d}$
MeC≡P	-20(15)	-10.76(48)	909(38)	86(39)	-581(38)	243(39)	-32(22)	824(54)
HC≡P	—	-43.64(15) <sup>60</sup>	961.1	74.1(9.8)	-632.8	254.3(9.8)	-41.4(3.3)	887.0(9.8)
N≡P	—	-78.2(5) <sup>61</sup>	961.1	-397.1(8.7)	-632.8	725.4(8.7)	272.7(2.9)	1358.4(8.7)
MeC≡P <sup>e</sup>					-402.31(64)	112.59(64)	-59.04(64)	514.90(91)
<sup>1</sup> AdC≡P <sup>f</sup>					-370.24(21)	87.09(21)	-65.35(21)	457.33(30)

<sup>a</sup> Calculated from the spin-rotation coupling constants using Flygare's diamagnetic shielding approximation and ground-state rotational constants,<sup>21,51,60,62</sup> except for the values from MAS SSNMR spectra. <sup>b</sup> Units of kHz. <sup>c</sup> Units of ppm. <sup>d</sup>  $\Omega = \delta_{\perp} - \delta_{\parallel}$ . <sup>e</sup> From a  $^{31}\text{P}$  MAS SSNMR spectrum of a frozen solution of MeC≡P in toluene. <sup>f</sup> From a  $^{31}\text{P}$  MAS SSNMR spectrum of the neat solid.

RIJCOSX-PBE0/pcSseg-3<sup>36,74-76</sup> level of theory:  $\delta_{11} = \delta_{22} = 148$  ppm,  $\delta_{33} = -488$  ppm,  $\delta_{\text{iso}} = -64$  ppm, and  $\Omega = 636$  ppm. This is another indication of the narrowing of the chemical shift anisotropy due to intermolecular interactions and molecular movement within the plastic crystal, resulting in partial rotational averaging of the observed CSA on the NMR timescale (*ca.* 10 ms).

We were also able to observe MeCP directly in frozen toluene solution at 103 K. Although the signal-to-noise level was low after 182 h of data acquisition, the  $^{31}\text{P}$  chemical shift tensor could be fitted to be  $\delta_{11} = \delta_{22} = 112.59(64)$  ppm,  $\delta_{33} = -402.31(64)$  ppm, indicating an isotropic shift of  $\delta_{\text{iso}} = -59.04(64)$  ppm and a span of  $\Omega = 514.90(91)$  ppm (Figure 4b). This chemical shift tensor is also smaller than the gas phase value from rotational spectroscopy, an effect that is likely due to similar solvent interactions and reorganizational motion when frozen into glassy toluene, such interactions being a dominant relaxation mechanism in low temperature MAS SSNMR.<sup>77</sup> Thus, the  $^{31}\text{P}$  nuclear spin-rotation coupling constant has provided a  $^{31}\text{P}$  CSA free from environmental influences, differing from the measurement by SSNMR in frozen toluene solution due to sensitivity to the medium.

## Conclusions

We anticipate this series of phosphaalkyne precursors to prove useful in any synthetic context tolerant of anthracene and triphenylphosphine coproducts, or else to be used in conjunction with vacuum transfer of the resulting  $\text{RC}\equiv\text{P}$  species. The thermolysis of **1-H** in the presence of CHD has shown anthracene release to precede triphenylphosphine release, more directly implicating an intermediate ylide-substituted phosphinidene. Our rotational spectra of MeC≡P from **1-Me** also demonstrate the continued promise of RPA compounds as sources of reactive species for spectroscopic investigations. Measurement of the gas phase  $^{31}\text{P}$  nuclear spin-rotation coupling tensor has provided a straightforward value for the CSA without influence of molecular motion or solvent interactions in the solid state.

**Acknowledgement** This material is based on research supported by the NSF grants CHE-1664799 and CHE-1566266, and the AFOSR grant FA9550-16-1-0117. T.J.B. thanks the NSF for a graduate research fellowship under grant 1122374. DNP/LTMAS NMR spectrometer time was kindly provided by Bruker Biospin Corp., Billerica, MA, USA.

**Supporting Information Available** Experimental details, characterization data, X-ray crystallographic information, computational details, and tables of Cartesian coordinates are provided in the Supporting Information document.

## References

- Regitz, M.; Scherer, O. J. *Multiple Bonds and Low Coordination in Phosphorus Chemistry*, 1st ed.; Thieme Publishing Group, 1990.
- Regitz, M.; Binger, P. Phosphaalkynes—Syntheses, Reactions, Coordination Behavior [New Synthetic Methods (73)]. *Angew. Chem. Int. Ed. Engl.* **1988**, *27*, 1484–1508.
- Nixon, J. F. Coordination chemistry of compounds containing phosphorus–carbon multiple bonds. *Chem. Rev.* **1988**, *88*, 1327–1362.
- Chirila, A.; Wolf, R.; Chris Slootweg, J.; Lammertsma, K. Main group and transition metal-mediated phosphaalkyne oligomerizations. *Coord. Chem. Rev.* **2014**, *270–271*, 57–74.
- Gier, T. E. HCP, A Unique Phosphorus Compound. *J. Am. Chem. Soc.* **1961**, *83*, 1769–1770.
- Hopkinson, M. J.; Kroto, H. W.; Nixon, J. F.; Simmons, N. P. C. The detection of the reactive molecule 1-phosphapropyne,  $\text{CH}_3\text{CP}$ , by microwave spectroscopy. *Chem. Phys. Lett.* **1976**, *42*, 460–461.
- Pellerin, B.; Denis, J.-M.; Perrocheau, J.; Carrie, R. Unhindered phosphaalkenes and phosphaalkynes in stable condition from a vacuum multistep sequence. *Tetrahedron Lett.* **1986**, *27*, 5723–5726.
- Guillemin, J. C.; Janati, T.; Denis, J. M.; Guenot, P.; Savignac, P. Synthesis of Nonstabilized Phosphaalkynes by Vacuum Gas-Solid HCl Elimination. *Angew. Chem. Int. Ed. Engl.* **1991**, *30*, 196–198.
- Guillemin, J.-C.; Janati, T.; Denis, J.-M. Lewis base-induced rearrangement of primary ethyn-1-ylphosphines, a new and efficient route to phosphaalkynes. *J. Chem. Soc., Chem. Commun.* **1992**, *0*, 415–416.
- Haber, S.; Flöch, P. L.; Mathey, F. Synthesis of phosphapropyne by flash thermolysis of 1-vinylphosphirane or divinylphosphine. *J. Chem. Soc., Chem. Commun.* **1992**, *0*, 1799–1800.
- Bock, H.; Bankmann, M. Thermische HCl-Abspaltung aus Alkyldichlorphosphanen  $(\text{H}_3\text{C}/\text{H})_3\text{C}-\text{PCl}_2$  zu Phosphaalkenen  $(\text{H}_3\text{C}/\text{H})_2\text{C}-\text{PCl}$  und Phosphaalkinen  $(\text{H}_3\text{C}/\text{H})\text{C}\equiv\text{P}$ . *Z. Anorg. Allg. Chem.* **1994**, *620*, 418–430.
- Guillemin, J.-C.; Janati, T.; Denis, J.-M. A Simple Route to Kinetically Unstabilized Phosphaalkynes. *J. Org. Chem.* **2001**, *66*, 7864–7868.
- Bergsträßer, U. *Science of Synthesis, Category 3, Compounds with Four and Three Carbon Heteroatom Bonds*; Thieme Verlag, 2004; pp 427–444.
- Regitz, M. Phosphaalkynes: new building blocks in synthetic chemistry. *Chem. Rev.* **1990**, *90*, 191–213.
- Mó, O.; Yáñez, M.; Guillemin, J.-C.; Riague, E. H.; Gal, J.-F.; María, P.-C.; Dubin Poliart, C. The Gas-Phase Acidity of HCP,  $\text{CH}_3\text{CP}$ , HCAs, and  $\text{CH}_3\text{CAs}$ : An Unexpected Enhanced Acidity of the Methyl Group. *Chem. Eur. J.* **2002**, *8*, 4919–4924.
- Jones, C.; Schulten, C.; Stasch, A. The first complexes and cyclodimerisations of methylphosphaalkyne (PC≡Me). *Dalton Trans.* **2006**, *0*, 3733–3735.
- Jones, C.; Schulten, C.; Stasch, A. Synthesis, Characterization and Reactivity of a  $\eta^1$ -Methylphosphaalkyne Complex,  $[\text{RuH}(\text{dppe})_2(\eta^1\text{-P}\equiv\text{CMe})][\text{CF}_3\text{SO}_3]$ . *Eur. J. Inorg. Chem.* **2008**, *2008*, 1555–1558.
- Cooper, T. A.; Kroto, H. W.; Nixon, J. F.; Ohashi, O. Detection of C-cyanophosphaethyne, NC–CP, by microwave spectroscopy. *J. Chem. Soc., Chem. Commun.* **1980**, *0*, 333–334.
- Kroto, H. W.; Nixon, J. F.; Simmons, N. P. C. The microwave spectrum of C-fluorophosphaethyne FC≡P: Structure determini-

nation, dipole moment, and vibration-rotation data. *J. Mol. Spectrosc.* **1980**, *82*, 185–192.

(20) Kroto, H. W.; Nixon, J. F.; Ohno, K.; Simmons, N. P. C. The microwave spectrum of phosphaethene,  $\text{CH}_2=\text{PH}$ . *J. Chem. Soc., Chem. Commun.* **1980**, *0*, 709.

(21) Kroto, H. W.; Nixon, J. F.; Simmons, N. P. C. The microwave spectrum of 1-phosphapropyne,  $\text{CH}_3\text{CP}$ : Molecular structure, dipole moment, and vibration-rotation analysis. *J. Mol. Spectrosc.* **1979**, *77*, 270–285.

(22) Westwood, N. P. C.; Kroto, H. W.; Nixon, J. F.; Simmons, N. P. C. Formation of 1-phosphapropyne,  $\text{CH}_3\text{CP}$ , by pyrolysis of dichloro-(ethyl)phosphine: a  $\text{He}(\text{I})$  photoelectron spectroscopic study. *J. Chem. Soc., Dalton Trans.* **1979**, *0*, 1405–1408.

(23) Kroto, H. W.; Nixon, J. F.; Simmons, N. P. C.; Westwood, N. P. C. FCP, *C*-fluorophosphaethyne: preparation and detection by photoelectron and microwave spectroscopy. *J. Am. Chem. Soc.* **1978**, *100*, 446–448.

(24) Hopkinson, M. J.; Kroto, H. W.; Nixon, J. F.; Simmons, N. P. C. The detection of unstable molecules by microwave spectroscopy: phospha-alkenes  $\text{CF}_2\text{PH}$ ,  $\text{CH}_2\text{PCl}$ , and  $\text{CH}_2\text{PH}$ . *J. Chem. Soc., Chem. Commun.* **1976**, *0*, 513–515.

(25) Transue, W. J.; Velian, A.; Nava, M.; Martin-Drumel, M.-A.; Womack, C. C.; Jiang, J.; Hou, G.-L.; Wang, X.-B.; McCarthy, M. C.; Field, R. W.; Cummins, C. C. A Molecular Precursor to Phosphaethyne and Its Application in Synthesis of the Aromatic 1,2,3,4-Phosphatriazolate Anion. *J. Am. Chem. Soc.* **2016**, *138*, 6731–6734.

(26) Bestmann, H. J.; Stransky, W.; Vostrowsky, O. Reaktionen mit Phosphanalkylenen, XXXIII. Darstellung lithiumsalzfreier Ylidlösungen mit Natrium-bis(trimethylsilyl)amid als Base. *Chem. Ber.* **1976**, *109*, 1694–1700.

(27) Anderson, S. P.; Goldwhite, H.; Ko, D.; Letsou, A.; Esparza, F. The nature of the carbon–phosphorus bond in methylidynephosphine. *J. Chem. Soc., Chem. Commun.* **1975**, *0*, 744–745.

(28) Wrackmeyer, B. Vergleich der NMR-Parameter von Phosphaalkinen und Nitrilen. *Z. Naturforsch. B* **1988**, *43*, 923–926.

(29) Levy, G. C.; Komoroski, R. A. Paramagnetic relaxation reagents. Alternatives or complements to lanthanide shift reagents in nuclear magnetic resonance spectral analysis. *J. Am. Chem. Soc.* **1974**, *96*, 678–681.

(30) Transue, W. J.; Velian, A.; Nava, M.; García-Iriepa, C.; Temprado, M.; Cummins, C. C. Mechanism and Scope of Phosphinidene Transfer from Dibenzo-7-phosphanorbornadiene Compounds. *J. Am. Chem. Soc.* **2017**, *139*, 10822–10831.

(31) Neese, F. The ORCA program system. *WIREs Comput. Mol. Sci.* **2012**, *2*, 73–78.

(32) Neese, F. Software update: the ORCA program system, version 4.0. *WIREs Comput. Mol. Sci.* **2018**, *8*, e1327.

(33) Zhao, Y.; Truhlar, D. G. The M06 suite of density functionals for main group thermochemistry, thermochemical kinetics, non-covalent interactions, excited states, and transition elements: two new functionals and systematic testing of four M06-class functionals and 12 other functionals. *Theor. Chem. Acc.* **2008**, *120*, 215–241.

(34) Weigend, F.; Ahlrichs, R. Balanced basis sets of split valence, triple zeta valence and quadruple zeta valence quality for H to Rn: Design and assessment of accuracy. *Phys. Chem. Chem. Phys.* **2005**, *7*, 3297–3305.

(35) Barone, V.; Cossi, M. Quantum Calculation of Molecular Energies and Energy Gradients in Solution by a Conductor Solvent Model. *J. Phys. Chem. A* **1998**, *102*, 1995–2001.

(36) Neese, F.; Wennmohs, F.; Hansen, A.; Becker, U. Efficient, approximate and parallel Hartree–Fock and hybrid DFT calculations. A ‘chain-of-spheres’ algorithm for the Hartree–Fock exchange. *Chem. Phys.* **2009**, *356*, 98–109.

(37) Weigend, F. Accurate Coulomb-fitting basis sets for H to Rn. *Phys. Chem. Chem. Phys.* **2006**, *8*, 1057–1065.

(38) Liu, L. L.; Zhou, J.; Andrews, R.; Stephan, D. W. A Room-Temperature-Stable Phosphanorcaradiene. *J. Am. Chem. Soc.* **2018**, *140*, 7466–7470.

(39) Baldwin, J. E.; Leber, P. A. Molecular rearrangements through thermal [1,3] carbon shifts. *Org. Biomol. Chem.* **2007**, *6*, 36–47.

(40) Herges, R. Coarctate and Pseudocoarctate Reactions: Stereocchemical Rules. *J. Org. Chem.* **2015**, *80*, 11869–11876.

(41) The data<sup>25</sup> used in the Eyring analysis of 1-H have been reprocessed using the same methodology as 1-Me as described in the SI.

(42) Glendening, E. D.; Badenhoop, J. K.; Reed, A. E.; Carpenter, J. E.; Bohmann, J. A.; Morales, C. M.; Landis, C. R.; Weinhold, F. NBO 6.0 (Theoretical Chemistry Institute, University of Wisconsin, Madison, 2013).

(43) Liu, L.; Ruiz, D. A.; Munz, D.; Bertrand, G. A Singlet Phosphinidene Stable at Room Temperature. *Chem* **2016**, *1*, 147–153.

(44) Velian, A.; Cummins, C. C. Synthesis and characterization of  $\text{P}_2\text{N}_3^+$ : An aromatic ion composed of phosphorus and nitrogen. *Science* **2015**, *348*, 1001–1004.

(45) Woerner, F. P.; Reimlinger, H. 1.5-Dipolare Cyclisierungen, II.  $\nu$ -Triazole aus Vinylaziden sowie durch Addition des Azid-Ions an die CC-Dreifachbindung. *Chem. Ber.* **1970**, *103*, 1908–1917.

(46) Höltzl, T.; Veszprémi, T.; Nguyen, M. T. Phosphaethyne polymers are analogues of cis-polyacetylene and graphane. *Compt. Rend.* **2010**, *348*, 1173–1179.

(47) Fuchs, E. P. O.; Hermesdorf, M.; Schnurr, W.; Rösch, W.; Heydt, H.; Regitz, M.; Binger, P. Ungewöhnlich koordinierte Phosphorverbindungen: XXIV. Methylidinphosphan (HCP), ein neuer Cycloadditionspartner für 1,3-Dipole. *J. Organomet. Chem.* **1988**, *338*, 329–340.

(48) St. Laurent, J. C. T. R. B.; Cooper, T. A.; Kroto, H. W.; Nixon, J. F.; Ohashi, O.; Ohno, K. The detection of some new phosphalkynes, RCP, using microwave spectroscopy. *J. Mol. Struct.* **1982**, *79*, 215–220.

(49) Ohno, K.; Yamamoto, Y.; Matsuura, H.; Murata, H. Infrared study on the  $\text{C}\equiv\text{P}$  stretching vibration of 1-phosphapropyne  $\text{CH}_3\text{C}\equiv\text{P}$  and its perdeuterium analog  $\text{CD}_3\text{C}\equiv\text{P}$ . *Chem. Lett.* **1984**, *13*, 413–414.

(50) Ohno, K.; Matsuura, H. The  $v_8$  Infrared Band of Ethyldynephosphine  $\text{CH}_3\text{C}\equiv\text{P}$  and Its Perdeuteride  $\text{CD}_3\text{C}\equiv\text{P}$ . *Bull. Chem. Soc. Japan* **1987**, *60*, 2265–2267.

(51) Bizzocchi, L.; Cludi, L.; Degli Esposti, C. Accurate quartic and sextic centrifugal distortion constants of  $\text{CH}_3\text{CP}$ . *J. Mol. Spectrosc.* **2003**, *218*, 53–57.

(52) Peterson, K. A.; Dunning, T. H. Accurate correlation consistent basis sets for molecular core–valence correlation effects: The second row atoms Al–Ar, and the first row atoms B–Ne revisited. *J. Chem. Phys.* **2002**, *117*, 10548–10560.

(53) Dunning, T. H. Gaussian basis sets for use in correlated molecular calculations. I. The atoms boron through neon and hydrogen. *J. Chem. Phys.* **1989**, *90*, 1007–1023.

(54) CFOUR, Coupled-Cluster techniques for Computational Chemistry, a quantum-chemical program package by J. F. Stanton, J. Gauss, M. E. Harding, P. G. Szalay with contributions from A. A. Auer, R. J. Bartlett, U. Benedikt, C. Berger, D. E. Bernholdt, Y. J. Bomble, L. Cheng, O. Christiansen, F. Engel, R. Faber, M. Heckert, O. Heun, C. Huber, T.-C. Jagau, D. Jonsson, J. Jusélius, K. Klein, W. J. Lauderdale, F. Lipparini, D. A. Matthews, T. Metzroth, L. A. Mück, D. P. O’Neill, D. R. Price, E. Prochnow, C. Puzzarini, K. Ruud, F. Schiffmann, W. Schwalbach, C. Simmons, S. Stopkowicz, A. Taiti, J. Vázquez, F. Wang, J. D. Watts and the integral packages MOLECULE (J. Almlöf and P. R. Taylor), PROPS (P. R. Taylor), ABACUS (T. Helgaker, H. J. Aa. Jensen, P. Jørgensen, and J. Olsen), and ECP routines by A. V. Mitin and C. van Wüllen. For the current version, see <http://www.cfour.de>.

(55) Faucher, A.; Wasylshen, R. E. In *Gas Phase NMR*; Jackowski, K., Jaszuński, M., Eds.; Royal Society of Chemistry: Cambridge, UK, 2016; pp 52–94.

(56) Ramsey, N. F. *Molecular Beams*; Oxford University Press, 1956.

(57) Pyykkö, P. Perspective on Norman Ramsey’s theories of NMR chemical shifts and nuclear spin–spin coupling. *Theor. Chem. Acc.* **2000**, *103*, 214–216.

(58) Ramsey, N. F. Magnetic Shielding of Nuclei in Molecules. *Phys. Rev.* **1950**, *78*, 699–703.

(59) Ramsey, N. F. Chemical Effects in Nuclear Magnetic Resonance and in Diamagnetic Susceptibility. *Phys. Rev.* **1952**, *86*, 243–246.

(60) Bizzocchi, L.; Esposti, C. D.; Dore, L.; Puzzarini, C. Lamb-dip millimeter-wave spectroscopy of HCP: Experimental and theoretical determination of  $^{31}\text{P}$  nuclear spin–rotation coupling constant and magnetic shielding. *Chem. Phys. Lett.* **2005**, *408*, 13–18.

(61) Raymonda, J.; Klemperer, W. Molecular Beam Electric Resonance Spectrum of  $^{31}\text{P}^{14}\text{N}$ . *J. Chem. Phys.* **1971**, *55*, 232–233.

(62) Cazzoli, G.; Cludi, L.; Puzzarini, C. Microwave Spectrum of  $\text{P}^{14}$  and  $\text{P}^{15}\text{N}$ : Spectroscopic Constants and Molecular Structure. *J. Mol. Struct.* **2006**, *780–781*, 260–267.

(63) Malli, G.; Froese, C. Diamagnetic Susceptibilities Calculated from Numerical Hartree-Fock Wave Functions. *Int. J. Quantum Chem.* **1967**, *1*, S99–S101.

(64) Flygare, W. H. Spin–Rotation Interaction and Magnetic Shielding in Molecules. *J. Chem. Phys.* **1964**, *41*, 793–800.

(65) Flygare, W. H. Magnetic interactions in molecules and an analysis of molecular electronic charge distribution from magnetic parameters. *Chem. Rev.* **1974**, *74*, 653–687.

(66) Brown, J.; Carrington, A. *Rotational Spectroscopy of Diatomic Molecules*; Cambridge University Press: Cambridge, UK, 2003; pp 410–416.

(67) Jameson, C. J.; Gutowsky, H. S. Calculation of Chemical Shifts. I. General Formulation and the Z Dependence. *J. Chem. Phys.* **1964**, *40*, 1714–1724.

(68) Jameson, C. J.; De Dios, A.; Keith Jameson, A. Absolute shielding scale for  $^{31}\text{P}$  from gas-phase NMR studies. *Chem. Phys. Lett.* **1990**, *167*, 575–582.

(69) Duchamp, J. C.; Pakulski, M.; Cowley, A. H.; Zilm, K. W. Nature of the carbon–phosphorus double bond and the carbon–phosphorus triple bond as studied by solid-state NMR. *J. Am. Chem. Soc.* **1990**, *112*, 6803–6809.

(70) Wu, G.; Rovnyak, D.; Johnson, M. J. A.; Zanetti, N. C.; Musaev, D. G.; Morokuma, K.; Schrock, R. R.; Griffin, R. G.; Cummins, C. C. Unusual  $^{31}\text{P}$  Chemical Shielding Tensors in Terminal Phosphido Complexes Containing a Phosphorus–Metal Triple Bond. *J. Am. Chem. Soc.* **1996**, *118*, 10654–10655.

(71) Amoureaux, J. P.; Bee, M. Crystal structure of 1-cyanoadamantane,  $\text{C}_{10}\text{H}_{15}\text{CN}$ , in its plastic phase. *Acta Cryst. B* **1979**, *35*, 2957–2962.

(72) Brand, R.; Lunkenheimer, P.; Loidl, A. Relaxation dynamics in

plastic crystals. *J. Chem. Phys.* **2002**, *116*, 10386–10401.

(73) Amoureaux, J. P.; Castelain, M.; Bee, M.; Arnaud, B.; Shouette-ten, M. L. An NMR Study of Molecular Motions in the Plastic Phases of 1-Cyanoadamantane. *Mol. Phys.* **1981**, *42*, 119–127.

(74) Adamo, C.; Barone, V. Toward reliable density functional methods without adjustable parameters: The PBE0 model. *J. Chem. Phys.* **1999**, *110*, 6158–6170.

(75) Jensen, F. Segmented Contracted Basis Sets Optimized for Nuclear Magnetic Shielding. *J. Chem. Theory Comput.* **2015**, *11*, 132–138.

(76) Stoychev, G. L.; Auer, A. A.; Neese, F. Automatic Generation of Auxiliary Basis Sets. *J. Chem. Theory Comput.* **2017**, *13*, 554–562.

(77) Lewandowski, J. R.; Halse, M. E.; Blackledge, M.; Emsley, L. Direct observation of hierarchical protein dynamics. *Science* **2015**, *348*, 578–581.